SECTION III. TASK 3. COMPREHENSIVE MODEL DEVELOPMENT AND EVALUATION

Objectives

The objective of this task is to integrate advanced chemistry and physics submodels into a comprehensive two-dimensional model of entrained-flow reactors (PCGC-2) and to evaluate the model by comparing with data from well-documented experiments. Approaches for the comprehensive modeling of fixed-bed reactors will also be reviewed and evaluated and an initial framework for a comprehensive fixed-bed code will be employed after submission of a detailed test plan (Subtask 3.b).

Task Outline

This task will be performed in three subtasks. The first covering the full 60 months of the program will be devoted to the development of the entrained-bed code. The second subtask for fixed-bed reactors will be divided into two parts. The first part of 12 months will be devoted to reviewing the state-of-the-art in fixed-bed reactors. This will lead to the development of the research plan for fixed-bed reactors. After approval of the research plan, the code development would occupy the remaining 45 months of the program. The third subtask to generalize the entrained-bed code to fuels other than dry pulverized coal would be performed during the last 24 months of the program.

III.A. SUBTASK 3.A. - INTEGRATION OF ADVANCED SUBMODELS INTO ENTRAINED-FLOW CODE, WITH EVALUATION AND DOCUMENTATION

Senior Investigators - B. Scott Brewster and L. Douglas Smoot
Brigham Young University
Provo, UT 84602
(801) 378-6240 and 4326

Research Assistants - Susana K. Berrondo and Gregg Shipp

Objectives

The objectives of this subtask are 1) to improve an existing 2-D code (PCGC-2) for entrained coal combustion and gasification to be more generally applicable to variation in coal rank and operating conditions by incorporating advanced coal chemistry submodels, advanced numerical methods, and an advanced pollutant submodel for both sulfur and nitrogen species, and 2) to validate the improved code. The improved code should be user-friendly and operate with reasonable run-times on a desk-top, engineering workstation.

Approach

The approach being followed is to 1) incorporate and evaluate advanced, coal-general and pollutant submodels being developed under Task 2 into PCGC-2, 2) improve code robustness and user-friendliness, and 3) implement the improved code on a workstation with a graphical user interface. Accomplishments during the last quarter are described below.

Accomplishments

Work continued on the integration and evaluation of the FG-DVC submodel in PCGC-2 and on improving code robustness. Work was also initiated on developing a graphical user interface.

Integration and Evaluation of the FG-DVC Submodel

A systematic approach was outlined in the 10th Quarterly Report (Solomon et al., 1989) for improving the FG-DVC submodel integration. This approach calls for investigating the relative effects of variability in offgas composition and enthalpy in order to determine the need for multiple solids

progress variables. Specifically, previous calculations (reported in the 6th Quarterly Report, Solomon et al., 1988) demonstrating the significance of separately tracking coal volatiles and char oxidation offgas were to be repeated with the FG-DVC submodel and full energy equation solution. These calculations were initiated during the past quarter. Problems were encountered in code convergence, and several code changes have been made. With these changes, a converged solution has been obtained for the case of a single solids progress variable with the FG-DVC submodel and a full energy equation solution. The results of this calculation will be reported in the next quarterly report, after results for the two-solids-progress-variable case have been obtained for comparison.

One of the problems encountered during the past quarter is that the residual char fraction calculated by the FG-DVC submodel did not seem to match the residual char fraction calculated by PCGC-2. It was thought that this might be related to the frequency of calling the FG-DVC submodel, or to the fact that PCGC-2 uses a predictor-corrector method for calculating the particle trajectory, whereas FG-DVC can only be called once for each time step. However, calling FG-DVC at every time step and using a simple Euler method in PCGC-2 did not seem to affect the result, and this problem is still under investigation. A streamlined version of FG-DVC, with extraneous variables removed from the code, is expected from AFR next quarter, and the calculation of residual char fraction will be investigated with the new submodel code version.

Work continued on the simulation of the transparent-wall reactor at AFR for submodel evaluation. The goal is to develop a definitive comparison, based on experimental data, of the FG-DVC submodel with other devolatilization submodels. Previous reports have described the comparison of simulation results with experimental data. Predictions assuming turbulent flow, based on an assumed inlet turbulence intensity of 10 percent have shown good agreement with the data for combustion of Montana Rosebud coal, even though the reactor was previously thought to be laminar. These calculations have been repeated with assumed intensities of 5 and 15 percent to see the effect of the assumed intensity. The results are shown in Figure III.A-1. Predictions assuming pure laminar flow are also shown for comparison. The FG-DVC submodel was used for the devolatilization rate in these calculations, and experimental data are also shown.

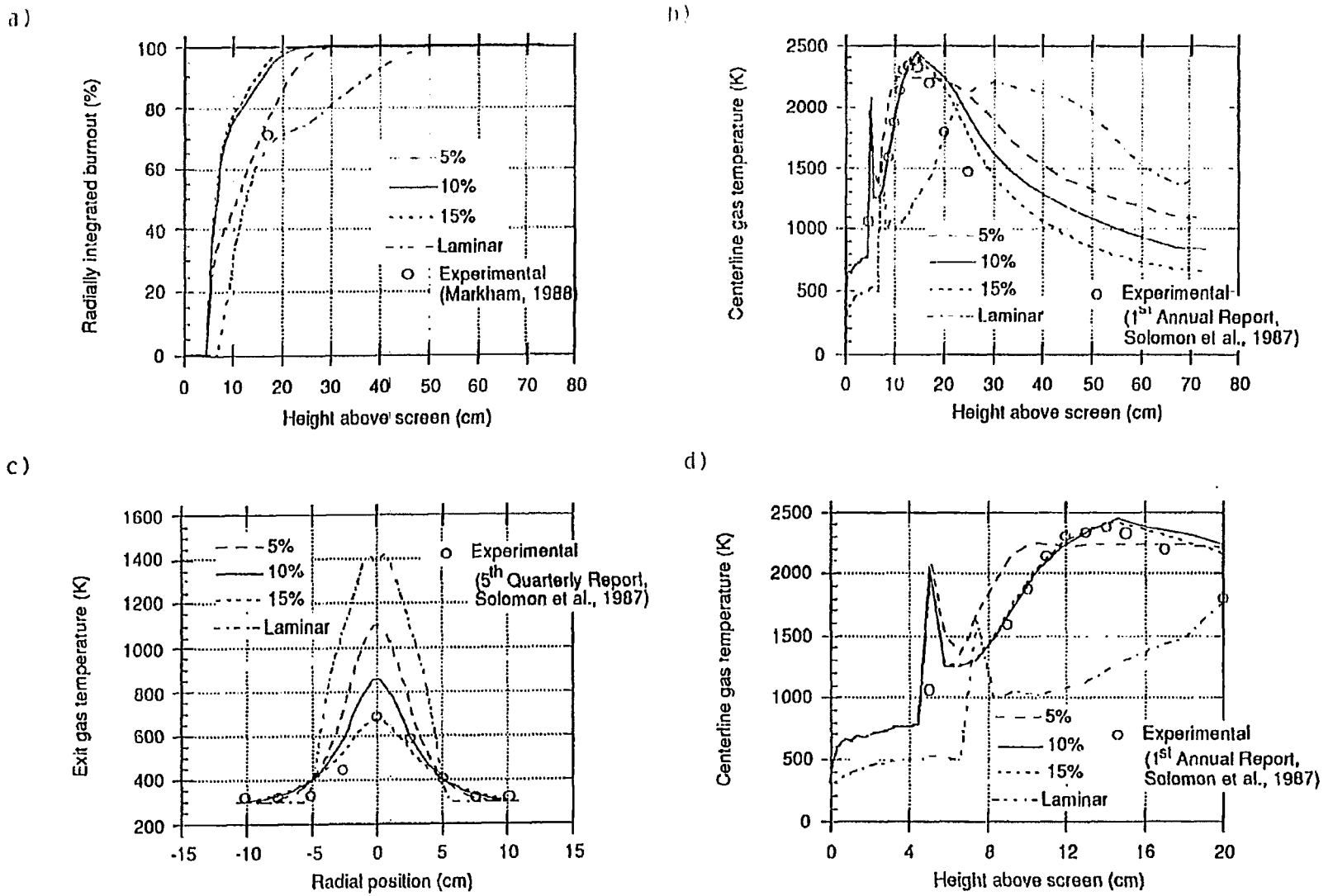

Figure III.A-1. Effect of inlet turbulence intensity on a) particle burnout, b) centerline gas temperature profile, and c) exit gas temperature profile, for combustion of Montana Rosebud coal. Figure d) is the same as b) with the region surrounding the flame front expanded.

The results in Figure III.A-1 show that the code predictions are generally sensitive to the assumed turbulence intensity. The location of the flame front is not sensitive to turbulence intensity; however, it is sensitive to whether the flow is turbulent or laminar. The temperature data agree more closely with the turbulent predictions. The single data point for burnout agrees equally well with the laminar prediction and the turbulent prediction with 6 percent inlet intensity. It is concluded, based on the temperature comparisons, that turbulent mixing is playing an important role in the reactor, and future efforts will focus on using PCGC-2 as a tool to help modify the reactor geometry and/or conditions to achieve laminar flow. Laminar flow data would provide a useful evaluation of the submodel because the uncertainties associated with turbulence would be absent. Additional simulations will also be carried out for a different coal, e.g. Pittsburgh No. 8.

Code Robustness

Another problem encountered during the past quarter is that the FG-DVC submodel was never called for smaller particles that experience periods of very low (or even negative) heating rate prior to devolatilization. These particles were heated to high temperatures (2000 K) and passed completely through the reactor without reacting. Small particles experience periods of very low or negative heating rate when the initial solids temperature is significantly less than that of the gas. In this case, the temperature of the gas decreases prior to the flame front because the particles act as a heat sink. Since the thermal relaxation time is small for the smaller particles, their temperature initially increases as they achieve thermal equilibrium with the gas, then decreases as the temperature of the gas decreases further, and then increases as the flame front is approached. The heating rate is therefore large initially, then decreases and goes negative, and then becomes large again. The time step for calling the FG-DVC submodel is calculated in PCGC-2 assuming that the particle temperature increases monotonically, with a fairly constant heating rate. In the case of the small particles entering the reactor at a temperature colder than the gas, a very large time interval (larger than the residence time of the particles in the reactor) was calculated when the heating rate became close to zero, and the FG-DVC submodel was never called.

A robust method of determining the time interval for calling the FG-DVC submodel has not been determined. Furthermore, it is not known how frequently

the submodel should be called for suitable accuracy. For the time being, the submodel is being called at every time step in the integration of the Lagrangian particle equations. The cpu time consumed by calling the submodel this frequently does not seem to be excessive, but consideration to improving the efficiency will be given at a later date.

Energy Equation

A subtle problem in the use of the full energy equation option became apparent during the last quarter and was partially solved. The problem became apparent when it was noticed that PCGC-2 was attempting to look up values in the gas physical properties table that were at temperatures much lower (as much as 200 degrees Kelvin) than the lowest temperature entering the reactor (300 K). Of course, such temperatures are physically unreasonable. The problem is apparently caused by an approximation in the method for calculating the time-average properties of the gas as a function of the local composition, enthalpy, and turbulence.

For any variable β, the time-averaged value $\tilde{\beta}$ is calculated by integrating the instantaneous value over the joint probability density function of the inlet gas mixture fraction f, the coal gas mixture fraction η, and the enthalpy h:

$$\tilde{\beta} = \int\int\int \beta(f,\eta,h)\tilde{P}(f,\eta,h)\,df\,d\eta\,dh \qquad \text{(III.A-1)}$$

The tilde (~) represents Favre averaging over time (weighted with density). The enthalpy is partitioned into the enthalpy h_a which is a function only of the mixing, and the residual enthalpy h_r (effects of radiation, expansion work, gas-to-particle convection, and non-adiabatic boundary conditions):

$$h = h_a + h_r = \eta h_c + (1-\eta)\left[f h_p + (1-f) h_s\right] + h_r \qquad \text{(III.A-2)}$$

h_c, h_p, and h_s are the enthalpies of the pure coal offgas, primary gas, and secondary gas, respectively. If the fluctuations of h_r are assumed small compared with the effects of the fluctuations of h_a, then Equation III.A-1 becomes

$$\bar{\beta} = \int_{-\infty}^{\infty}\int_{-\infty}^{\infty} \beta(\tilde{f},\eta,h_r)\tilde{P}(\tilde{f},\eta)d\tilde{f}d\eta \qquad \text{(III.A-3.}$$

where h_r is constant relative to the fluctuations in f and η.

Assuming a clipped Gaussian density function for $\tilde{P}$, and assuming $\tilde{P}(\tilde{f},\eta)$ is separable, Equation III.A-3 can be expanded. The result is shown in Table III.A-1, where α_p, α_s, α_c, and α_i represent the fraction of time a probe fixed in space would see pure primary gas, pure secondary gas, pure coal offgas, and pure inlet gas (no coal offgas), respectively. Historically, it has been argued that terms representing pure primary, secondary, or coal offgas (Eqs. III.A-7, 4, and 6, respectively) should be evaluated at h_r=0 because such eddies will occur only near the inlet and will have had little chance to gain or lose heat from the surroundings. Hence h should equal h_a for these eddies. This has been the assumption used in PCGC-2. However, a similar argument could also be made for the other terms involving incomplete mixing (i.e. Eqs. III.A-5, 8, and 9). Any eddy with incomplete mixing has probably had little thermal interaction with its environment and probably has an enthalpy equal to h_a. Evaluating the terms in Equations A-5, 8, and 9 at h_r=0 reduced the number of times the physical properties table was accessed at unreasonably low temperatures, but did not eliminate them. Some unreasonable attempts are due to the term representing fully mixed fluid, Equation III.A-10, which is the most important term. A suitable method of evaluating this term without table accesses at unreasonable temperatures has not been found, but the contribution to the value of the term by properties accessed at these low temperatures is probably insignificant.

Graphical User Interface

Previous reports have described the implementation of the code on several engineering workstations and mainframe computers. The use of two commercial graphics packages for viewing code output has also been described. During the last quarter, development of a graphical user interface on the Sun workstation was initiated. The interface will make it much simpler to interact with the program, both for input and output, and also for running the program and monitoring its progress.

TABLE III.A-1

TERMS RESULTING FROM EXPANSION OF EQUATION III.A-3

Term	Description	Equation no.
$\alpha_s\alpha_s\beta(0,0,h_r)$	Eddies of pure secondary gas	(III.A-4)
$\alpha_s\int_{0^+}^{1^-}\beta(0,\eta,h_r)\tilde{P}(\eta)d\eta$	Eddies with secondary and coal offgas but no primary gas	(III.A-5)
$\alpha_c\beta(f,1,h_r)$	Eddies of pure coal offgas	(III.A-6)
$\alpha_p\alpha_p\beta(1,0,h_r)$	Eddies of pure primary gas	(III.A-7)
$\alpha_p\int_{0^+}^{1^-}\beta(1,\eta,h_r)\tilde{P}(\eta)d\eta$	Eddies with primary and coal offgas but no secondary gas	(III.A-8)
$\alpha_1\int_{0^+}^{1}\beta(f,0,h_r)\tilde{P}(f)df$	Eddies with primary and secondary but no coal offgas	(III.A-9)
$\int_{0^+}^{1^-}\left[\int_{0^+}^{1^-}\beta(f,\eta,h_r)\tilde{P}(f)df\right]\tilde{P}(\eta)d\eta$	Eddies with primary, secondary and coal offgas	(III.A-10)

The interface takes advantage of the user interface toolkit available on the Sun-4 workstation. It is a graphics-based application that runs within windows. The user will be able to choose, by means of a menu, any data item from an input file for PCGC-2 and change it as needed. The basic code is being written in the C computer language with a Fortran driver that does all the reading and writing procedures. A main subroutine creates all the windows.

Figure III.A-2 shows a printout of the Sun workstation monitor with the PCGC-2 interface in operation. Different grouped variables, such as program controls, the dimensions of the reactor, and the under-relaxation factors, can be accessed from a panel in the base frame. Selecting "program controls" with the mouse, for example, causes a menu to pop out which has check marks on those controls that are selected (assigned as "true" in the input file). The user can alter the selection status by releasing the mouse button over a desired control feature. Choosing "dimensions" opens a window where the user can change the value of the reactor dimensions. Choosing "under-relaxation factors" opens a window where the under-relaxation factors can be altered by moving a slider button with the mouse.

In addition to the program which modifies code input, a code is being developed to run PCGC-2. This program obtains the required data files from the user and does all the file-handling procedures completely transparent to the user. That is, it cleans the working directory of possible leftover files and links the run-specific filenames to the internal names used by PCGC-2. The main program creates the base frame and a panel (shown in upper-right portion of Figure III.A-2) where the names of the files can be written. In this panel, there is a button used to start running PCGC-2 once the user has given names for the files. The program is then called with the names of the files as parameters.

Plans

During the next quarter, work will continue on integrating and evaluating the FG-DVC submodel in PCGC-2. A new, stream-lined code version of the FG-DVC submodel will be integrated and tested. The residual char fraction predicted by PCGC-2 and by the FG-DVC submodel will be compared. The need for multiple solids progress variables will be investigated by performing calculations with two solids progress variables and comparing the results with those using a single solids progress variable. Work will be initiated to

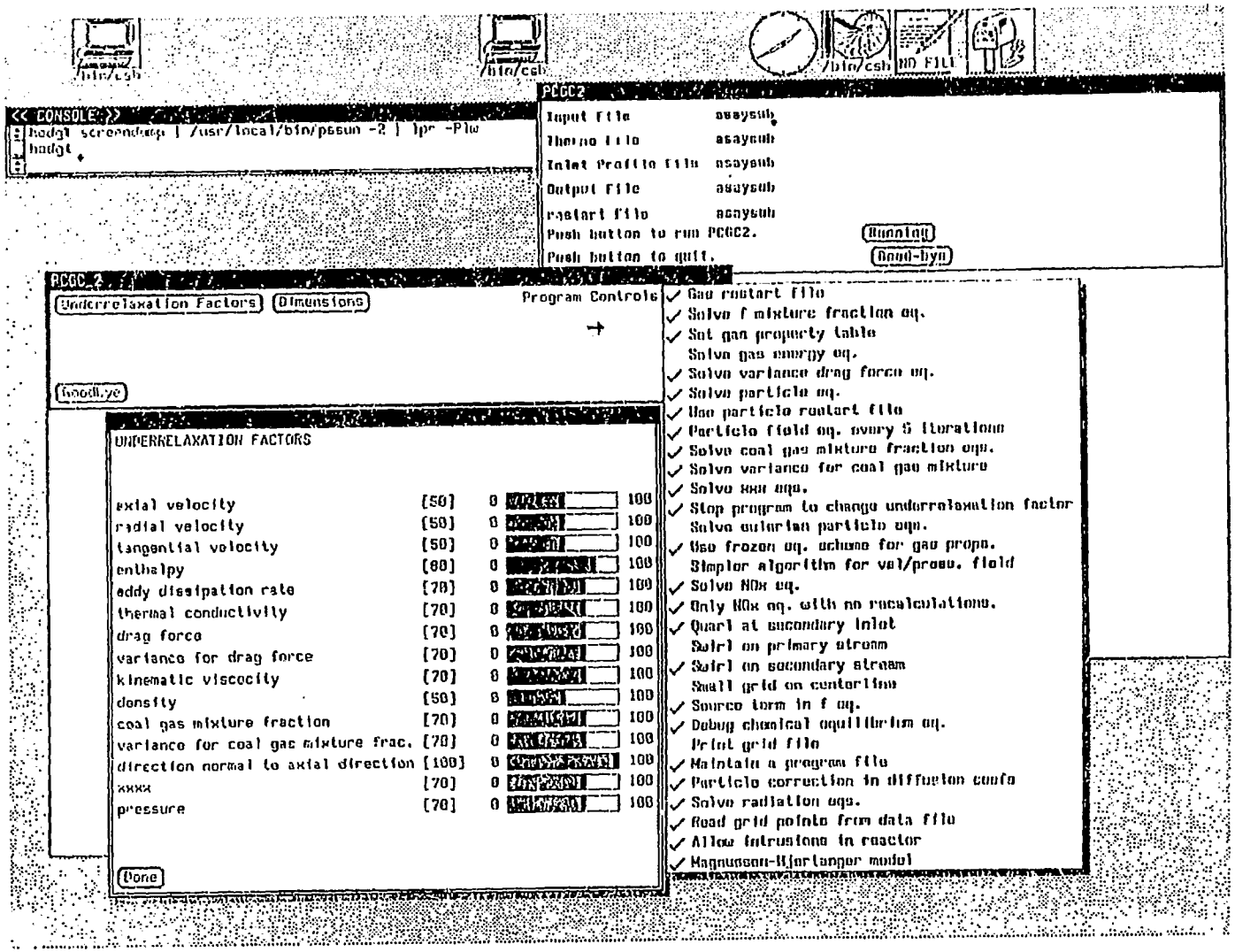

Figure III.A-2. Screen dump showing windows for PCGC-2 graphical user interface on Sun-4 workstation.

generalize the code to allow particles in any inlet. Work will continue on modeling the transparent-wall reactor and on evaluating the FG-DVC submodel. Simulations will be carried out for a different coal and for a char, and also for different reactor geometry and/or conditions to suggest modifications that might help achieve laminar flow in future experiments. Work will also continue on the development of the graphical user interface.

III.B. SUBTASK 3.B. - COMPREHENSIVE FIXED-BED MODELING REVIEW, DEVELOPMENT, EVALUATION, AND IMPLEMENTATION

Senior Investigators - Predrag T. Radulovic and L. Douglas Smoot
Brigham Young University
Provo, Utah 84602
(801) 378-3097 and (801) 378-4326

Graduate Research Assistant - Michael L. Hobbs

Objectives

The objectives of this subtask are: 1) to provide a framework for an advanced fixed-bed[1] model for incorporating the advanced submodels being developed under Task 2, particularly the large-particle submodel (Subtask 2.e.), and 2) to provide a basis for evaluating the advanced model. Development of the basic framework of the model and initial integration of the advanced submodels was completed during Phase I. During Phase II, the model and submodels will be improved, extended, and applied under Task 4 to systems of practical interest.

Accomplishments

During the last quarter, work continued on reviewing numerical techniques used in comprehensive fixed-bed models, obtaining validation data from the literature, and coding the chemical submodels. Three equilibrium-based, moving-bed chemical submodels were written, debugged, and partially validated. The three codes are based on total equilibrium, 1-zone partial equilibrium, and 2-zone partial equilibrium. The partial-equilibrium models use the functional group (FG) submodel to predict ultimate volatiles composition (including tar) and either the 2-step model or FG model to predict ultimate volatiles yield. The equilibrium models predict reasonable effluent properties and will be used to provide an initial guess for the 1-D moving-bed model. The development of the equilibrium-based, fixed-bed models has provided familiarity with the chemical submodels to be used in the 1-D moving-bed model, and has also provided insight into the moving-bed coal gasification process.

---

[1]The term "fixed bed" is in common usage although the bed is actually moving slowly. "Fixed bed" and "moving bed" are used here interchangeably.

Numerical Techniques

Solution Techniques - The general set of governing equations with appropriate assumptions was presented in the 10th Quarterly Report (Solomon et al., 1989). A compilation of selected moving-bed models from the literature that solve similar sets of equations is given in Table III.B-1. The selected models include the University of Delaware (UD) model (Yoon et al., 1977, 1978a, 1978b, 1979a, 1979b), the IBM model (Stillman, 1979), the WU model from Joseph and students at Washington University (Cho and Joseph, 1981; Kim and Joseph, 1983), the WV model from Wen and students at West Virginia University (Desai and Wen, 1978; Wen, 1982; Wen et al., 1982), the AS model used in the ASPEN flowsheeting system (Benjamin, 1985; Rinard and Benjamin, 1985; Rinard, et al., 1984; Stefano, 1985), and the LL model from Lawrence Livermore Laboratory (Winslow, 1976; Ronsa and Thorsness, 1976; Thorsness et al., 1978; Thorsness and Kang, 1984).

The solution techniques for the models listed in Table III.B-1 are all similar. A typical solution method for a homogeneous, steady-state char gasification model is as follows:

1. Assume a value for the carbon conversion in the solid output.

2. Integrate the set of ordinary differential equations from the bottom of the reactor to the top using a numerical technique such as Runge-Kutta.

3. Compare the carbon flow rate at the top of the reactor with the input carbon feed rate.

4. Repeat steps 1-3 until calculated input carbon equals actual carbon feed.

The heterogeneous models require an additional iteration loop for each integration step to calculate the particle temperature. If devolatilization is included, a third iteration loop is required (Cho, 1980).

The set of ordinary differential equations comprising the 1-D, moving-bed model form a split-boundary-value problem. All of the moving-bed models discussed in Table III.B-1, except the LL model, use Runge-Kutta methods to solve the initial-value problems. The LL model uses LSODE (stiff ODE solver

TABLE III.B-1

NUMERICAL SOLUTION TECHNIQUES FOR SELECTED 1-D MOVING-BED MODELS

Model	Year	Type[+]	Order[‡]	Integration Method
UD	1978	1-D, homogeneous, steady	B-T	5th order Runge-Kutta (Fibonacci search to match boundary conditions)
IBM	1979	1-D, heterogeneous, steady	T-B	5th order Runge-Kutta-Felberg variable step algorithm
WU	1981	1-D, heterogeneous, steady	B-T	4th order Runge-Kutta (Wegstein search to match boundary conditions)
WV	1982	1-D, homogeneous, steady	B-T	4th order Runge-Kutta (Secant method to match boundary conditions)
AS	1984	1-D, homogeneous, steady	B-T	Same as UD Model
LL	1984	1-D, heterogeneous, transient	N/A	LSODE solver

[+]Homogeneous refers to equal particulate and gas phase temperatures.
[‡]Order refers to the calculation order from top to bottom (T-B) or bottom to top (B-T).

TABLE III.B-2

TYPICAL VALUES FOR CONVECTIVE HEAT TRANSFER COEFFICIENTS[‡]

Convective Mechanism	$U, \frac{watts}{m^2 K}$
Free Convection	5-25
Forced Convetion (Gases)	25-250
Forced Convection (Liquids)	50-20,000
Convection with Phase Change	2,500-100,000
Well Mixed Temperature	800 K, 900 K, 1000 K, 1500K
$U, \frac{watts}{m^2 K}$ for Lurgi Mark II (See Figure III.B-1)	154, 116, 93, 47

[‡]Typical values are from Incropera and DeWitt (1981). Lurgi values are calculated assuming a jacket steam mass flow rate of 0.9 kg s^{-1}, heat transfer area of 35 m^2, and water wall temperature of 495 K.

developed at Lawrence Livermore National Laboratory, Hindmarsh, 1983) to solve the initial-value problem.

Consultation on Numerical Methods - Dr. Dov Bai at Utah State University was consulted with respect to solution techniques. Multigrid methods were suggested to treat steep temperature and concentration gradients. Dr. Bai also suggested practical debugging techniques which are being used in the 3-D pulverized code being developed at BYU. After the equation set and numerical integration routines are coded, the integrator and equation sets can be tested by assuming an analytical solution to the set of equations and by rewriting the source terms and boundary conditions to satisfy the assumed solution.

Evaluation Data

Moving-Bed Data - Experimental data are needed for model evaluation that provide a critical measure of the model's capability in predicting the detailed reactor performance. Detailed profile data of particle temperature, gas temperature, pressure, gas composition, and particle composition in the reactor bed are needed. Unfortunately, only limited detailed data exist, at least in the open literature. There are no published data available for separate gas and solids temperatures or gas composition in the bed. Effluent gas compositions and temperatures as well as limited temperature and pressure profile data may be used as a partial basis for model evaluation.

Detailed operational data on four American coals gasified in Lurgi Mark II reactors in Westfield, Scotland are available (Elgin and Perks, 1973, 1974). The Westfield data also include flare gas analysis and gas off-take temperature. The four coals are Illinois No. 6 (greatest reserve for Eastern caking coals), Illinois No. 5 (equivalent to Kentucky No. 9), Pittsburgh No. 8 (major Eastern coal with a very high swelling index), and Rosebud seam (subbituminous coal from South-Eastern Montana).

Figure III.B-1 gives operational data from the Illinois No. 6, Westfield, American coal tests. The Illinois No. 6 case at Westfield has been used to validate several fixed-bed models (e.g. Yoon et al., 1978b; Cho and Joseph, 1981; Kim and Joseph, 1983; Wen et al., 1982). The Rosebud case (data given in Elgin and Perks, 1974) has also been used for validation (Stillman, 1979; Wen et al., 1982). Data from Elgin and Perks was used as input for the equilibrium models discussed below.

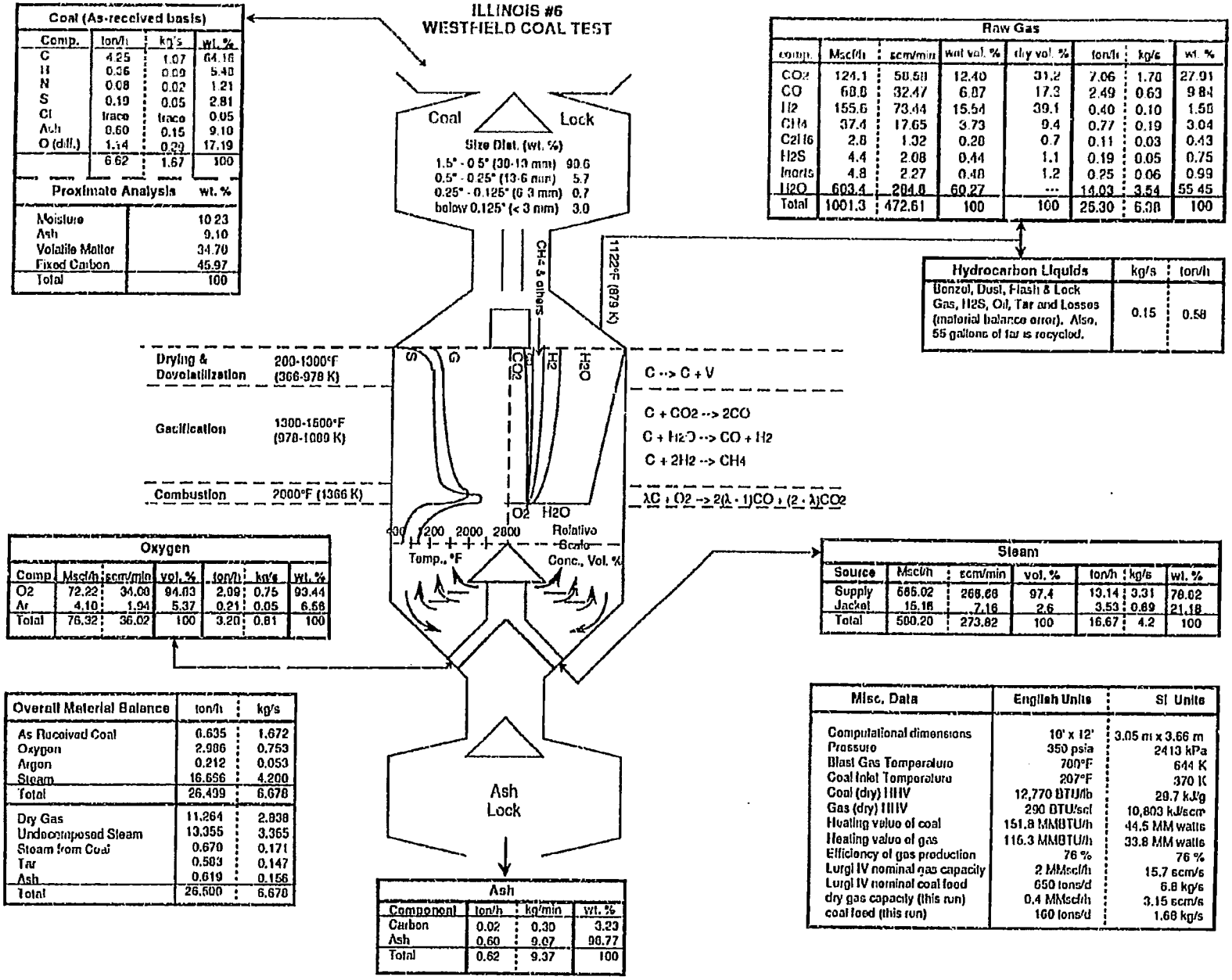

Coal (As-received basis)			
Comp.	ton/h	kg/s	wt. %
C	4.25	1.07	64.16
H	0.36	0.09	5.48
N	0.08	0.02	1.21
S	0.19	0.05	2.81
Cl	trace	trace	0.05
Ash	0.60	0.15	9.10
O (diff.)	1.14	0.29	17.19
	6.62	1.67	100

Proximate Analysis	wt. %
Moisture	10.23
Ash	9.10
Volatile Matter	34.70
Fixed Carbon	45.97
Total	100

Raw Gas							
comp.	Mscf/h	scm/min	wet vol. %	dry vol. %	ton/h	kg/s	wt. %
CO2	124.1	58.58	12.40	31.2	7.06	1.78	27.91
CO	68.8	32.47	6.87	17.3	2.49	0.63	9.84
H2	155.6	73.44	15.54	39.1	0.40	0.10	1.58
CH4	37.4	17.65	3.73	9.4	0.77	0.19	3.04
C2H6	2.8	1.32	0.28	0.7	0.11	0.03	0.43
H2S	4.4	2.08	0.44	1.1	0.19	0.05	0.75
Inerts	4.8	2.27	0.48	1.2	0.25	0.06	0.99
H2O	603.4	284.8	60.27	---	14.03	3.54	55.45
Total	1001.3	472.61	100	100	25.30	6.38	100

Hydrocarbon Liquids	kg/s	ton/h
Benzol, Dust, Flash & Lock Gas, H2S, Oil, Tar and Losses (material balance error). Also, 55 gallons of tar is recycled.	0.15	0.58

Oxygen						
Comp	Mscf/h	scm/min	vol. %	ton/h	kg/s	wt. %
O2	72.22	34.00	94.63	2.09	0.75	93.44
Ar	4.10	1.94	5.37	0.21	0.05	6.56
Total	76.32	36.02	100	3.20	0.81	100

Steam						
Source	Mscf/h	scm/min	vol. %	ton/h	kg/s	wt. %
Supply	485.02	266.66	97.4	13.14	3.31	78.02
Jacket	15.18	7.16	2.6	3.53	0.89	21.18
Total	500.20	273.82	100	16.67	4.2	100

Overall Material Balance	ton/h	kg/s
As Received Coal	6.635	1.672
Oxygen	2.986	0.753
Argon	0.212	0.053
Steam	16.666	4.200
Total	26.499	6.678
Dry Gas	11.264	2.838
Undecomposed Steam	13.355	3.365
Steam from Coal	0.670	0.171
Tar	0.583	0.147
Ash	0.619	0.156
Total	26.500	6.678

Misc. Data	English Units	SI Units
Computational dimensions	10' x 12'	3.05 m x 3.66 m
Pressure	350 psia	2413 kPa
Blast Gas Temperature	700°F	644 K
Coal Inlet Temperature	207°F	370 K
Coal (dry) HHV	12,770 BTU/lb	29.7 kJ/g
Gas (dry) HHV	290 BTU/scf	10,803 kJ/scm
Heating value of coal	151.8 MMBTU/h	44.5 MM watts
Heating value of gas	115.3 MMBTU/h	33.8 MM watts
Efficiency of gas production	76 %	76 %
Lurgi IV nominal gas capacity	2 MMscf/h	15.7 scm/s
Lurgi IV nominal coal feed	650 tons/d	6.8 kg/s
dry gas capacity (this run)	0.4 MMscf/h	3.15 scm/s
coal feed (this run)	160 tons/d	1.68 kg/s

Ash			
Component	ton/h	kg/min	wt. %
Carbon	0.02	0.30	3.23
Ash	0.60	9.07	96.77
Total	0.62	9.37	100

Figure III.B-1. Information data sheet for Illinois No. 6, at Westfield Scotland (data taken primarily from Elgin and Perks, 1974).

Equilibrium Chemical Submodels

An important submodel in the 1-D fixed-bed model is the chemical submodel. A significant effort has been initiated during the past quarter toward development of this submodel. The initial thrust has been on the gas phase component. Three different equilibrium options have been investigated and each is discussed below. While these submodel options are candidates for inclusion in the 1-D fixed-bed model, they also can be used as overall models for the entire fixed-bed process. Thus, the analyses shown below apply these chemical submodels to various fixed-bed processes.

Total Equilibrium Submodel

Background - Pratt and Wormeck (1976) have developed a code (CREE, Combustion Reaction Equilibrium for Elements) for complex equilibrium computations. CREE has been used at BYU for the 1, 2, and 3-dimensional pulverized-coal combustion codes. CREE is based on minimization of Gibbs free energy to determine equilibrium states at prescribed temperatures and pressures. Detail on multicomponent equilibrium calculations can be found in Pratt (1979).

Equilibrium terminology can be misleading when referring to different equilibrium assumptions. Various equilibrium assumptions will be briefly discussed for clarity. Fractional equilibrium involves multiplying the equilibrium constants by "approach factors" to match measured compositions. The choice of the approach factors is not based on any physical reasoning. Fractional equilibrium refers to the models by Gumz (1952), Woodmansee (1976), and Wen et al. (1982).

Partial equilibrium refers to letting certain reactions or species go to equilibrium while calculating other species by other means such as kinetics or by assuming no further reaction. In other words, partial equilibrium is assumed if any species is considered to be out of equilibrium. The non-equilibrium species concentrations may be found by using heterogeneous kinetics devolatilization, gasification, or oxidation) or homogeneous gas phase kinetics. Most moving-bed models in the literature have assumed the major gaseous species (CO, CO_2, H_2, and H_2O) to be in equilibrium by using the water-gas-shift reaction. Another approach is to assume selected minor species to be in equilibrium and to predict major species with homogeneous or

heterogeneous kinetics. Homogeneous kinetic modeling of CO out of equilibrium by assuming partial equilibrium has been demonstrated by Colson (1989).

The interface between kinetics and partial equilibrium should be clarified. The thermal interface can be easily treated by using a non-reacting species with an identical heat capacity in the equilibrium calculation. The concentration of the non-equilibrium species is then determined by the kinetic equations. The concentration interface is not so clearly defined. The presence of the non-equilibrium species can shift the equilibrium concentration. The effect of non-equilibrium species on equilibrium species may be negligible if the kinetic species concentration (non-equilibrium species concentration) is small. The effect of non-equilibrium species concentration is simulated by the non-reacting species which has a similar partial pressure as the reacting species but is not allowed to react.

Total equilibrium refers to all species being in equilibrium. If the total static enthalpy, pressure and atomic composition are known, the equilibrium composition can be determined. This is the assumption used in the total equilibrium model.

Model Assumptions - Figure III.B-2a shows the control volume used for the total equilibrium chemistry submodel. The ash temperature, well-mixed reactor temperature (or zero-dimensional temperature), and exit raw gas temperatures are assumed to be the same. The daf coal is also assumed to completely react. Complete reaction of the daf coal is equivalent to assuming the daf coal reacts completely either by devolatilization, gasification or oxidation. There is no differentiation in this submodel regarding the mechanism for these chemical processes.

The feed coal and blast gas composition, mass flow rate and temperature are input parameters. Reactor geometry is also specified by the user. The heat loss is determined by either specifying an overall heat transfer coefficient or by specifying the jacket steam flow rate. The wall temperature is assumed to be equal to the saturated steam temperature at the reactor operating pressure. The heating value of the coal is either specified in the input or calculated from the ultimate analysis using Dulong's formula (Reid et al., 1973).

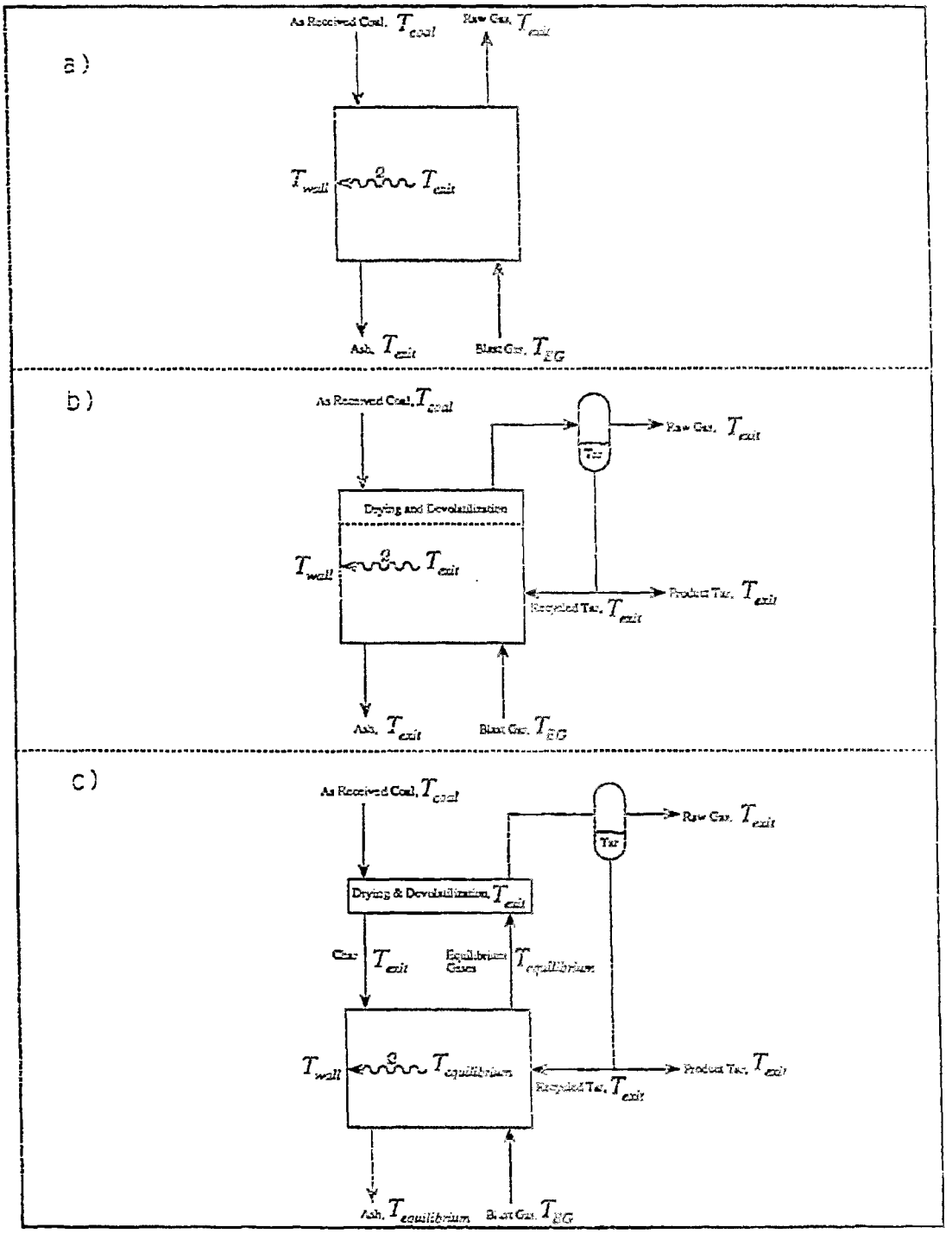

Figure III.8-2. Control volume for a) 1-zone total equilibrium model, b) 1-zone partial equilibrium model, and c) 2-zone partial equilibrium model.

Equations and Solution Technique - The exiting raw gas composition and temperature can be calculated by doing an overall energy and material balance on the control volume shown in Figure III.B-2a and assuming total equilibrium. The energy balance around the control volume in Figure III.B-2a is

$$\dot{m}_c h_c + \dot{m}_{bg} h_{bg} - \dot{m}_a h_a - \dot{m}_g h_g - Q = 0 \qquad \text{(III.B-1)}$$

where $\dot{m}$ and h refer to mass flow rate (kg/s) and total enthalpy (J/kg), respectively. The subscripts c, bg, a and g refer to raw coal, blast gas (steam and oxygen), ash and raw gas streams, respectively. The total enthalpy is composed of the formation enthalpy and the sensible enthalpy as shown below:

$$h = h_f^o + h^s \qquad \text{(III.B-2)}$$

where the superscripts o and s refer to the standard temperature (298.15 K) and sensible enthalpy from the reference temperature to the stream temperature. Equation III.B-1 can be solved for the total or static enthalpy of the gas, h_g, if the exit temperature is known. The solution technique is as follows:

1. Guess the exit temperature, T_e.
2. Calculate quantities that depend on T_e, (e.g. h_g, h_a^s, and Q).
3. Calculate T_e, by material balance and equilibrium assumption.
4. Repeat 1-3 until guessed T_e equals calculated T_e.

The solution technique described above requires the heat of formation of the daf coal. The heat of formation of coal, $h_{f,c}^o$, is based on the following reaction as given by the GPSA databook (1987):

$$C_n H_m O_n S_j N_k + \left(n + \tfrac{m}{4} - \tfrac{h}{2} + j\right) O_2 \rightarrow nCO_2 + \tfrac{m}{2} H_2O + \tfrac{k}{2} N_2 + jSO_2 \qquad \text{(III.B-3)}$$

The heat of formation of the coal can be obtained by noting that the heat of combustion, ΔH_c^o, is the negative of the higher heating value of the coal, HHV, which is an input parameter. The heat of combustion is determined as a difference of the heat of formation of the products and the heat of formation of the coal:

$$\Delta H_c^\circ = -HHV = \sum_{i=1}^{4} \nu_i \left(h_f^\circ\right)_i - h_{f,c}^\circ \qquad \text{(III.B-4)}$$

$$\text{or,} \qquad h_{f,c}^\circ = \sum_{i=1}^{4} \nu_i \left(h_f^\circ\right)_i + HHV \qquad \text{(III.B-5)}$$

where ν represents the stoichiometric coefficient for the i^{th} product given in Equation III.B-3 and $i = 1$-4 represents the formation of CO_2, $H_2O(l)$, N_2, and SO_2 respectively. The primary disadvantage of using Equation III.B-5 for calculating the heat of formation of coal is the error that results from computing a relatively small number as the difference of two much larger numbers that are of limited accuracy (Johnson, 1981). Calculations done for the Illinois No. 6 coal depicted in Figure III.B-1 give 170% error in the heat of formation calculation for ±5% error in the *HHV* measurement. Fortunately, the enthalpy of the feed coal is small in comparison to the blast gas enthalpy for dry-ash, moving-bed gasifiers and has little influence on the equilibrium calculations. Smith (1989) has also determined the impact of the heat of formation to be small for pulverized combustion cases. It is uncertain whether the heat of formation will have a significant influence for slagging gasifiers. These questions can be answered by future sensitivity analyses of the moving-bed model.

The heats of formation and sensible enthalpies for the blast gases are found using CREE which uses polynomial fits of the JANAF thermochemical tables (Stull and Prophet, 1971). The sensible enthalpies for the feed coal, h_c^s, can be determined using Merrick's enthalpy correlation (1983) to calculate enthalpy at the coal feed temperature (reference temperature is standard, 298.15 K):

$$h_c^s = \left(\frac{R}{a}\right)\left[380 g_o\left(\frac{380}{T}\right) + 3600 g_o\left(\frac{1800}{T}\right)\right] \left(\frac{J}{kg}\right) \qquad \text{(III.B-6)}$$

where

$$g_o(z) = \frac{1}{(\exp(z)-1)} \qquad \text{(III.B-7)}$$

and R = the gas constant (8314.4 J kmol^{-1} K^{-1}), T = solid temperature (K), 380 and 1800 are characteristic Einstein temperatures (K). The mean atomic weight, a, may be defined as:

$$\frac{1}{a} = \sum_{i=1}^{5} y_i \mu_i \qquad \text{(III.B-8)}$$

where μ_i represents the atomic weights of carbon, hydrogen, oxygen, nitrogen and sulphur, and y_i is the ultimate analysis of the coal. Following the suggestion of Merrick (1983), Kirov's correlation was used for the specific heat of the ash:

$$Cp_a = 754 + 0.856\,T\ (\tfrac{J}{kg\,K}),\ \text{where T(°C)} \qquad \text{(III.B-9)}$$

The final term to define in Equation III.B-4 is the heat loss through the reactor wall, Q. This quantity can be calculated directly, if the jacket steam flow rate is known, or by the following equation, if the overall heat transfer coefficient, U (watts m^{-2} K^{-1}), is known:

$$Q = UA(T_e - T_w) \qquad \text{(III.B-10)}$$

where A is the water wall surface area (m^2), T_e and T_w represent the well-mixed or exit temperature and water wall temperature, respectively. Typical values for U are shown in Table III.B-2. Values for the overall heat transfer coefficient, U, range from 50-200 watts m^{-2} K^{-1}. As shown in Table III.B-2, the overall heat transfer is in the forced convection range.

Total Equilibrium Submodel Results - The simple, total equilibrium submodel was written to test the equilibrium routines. Agreement between several equilibrium codes has been achieved with CREE, NASACEC (Gordon and McBride, 1976), and EDWARDS (Selph, 1965). The total equilibrium model has been evaluated using data obtained from the American coal tests done at Westfield, Scotland in a dry-ash Lurgi Mark II. Adequate compositions and temperatures have been predicted. The effect of steam flowrate on temperature and H_2O/CO molar ratio has also been investigated. As expected, the temperature decreased with increasing H_2O/O_2 ratio. Also, the H_2/CO ratio increased with increasing H_2O/O_2. The largest discrepancy is low carbon monoxide concentration in the product gas. The results of the total equilibrium model will be discussed in more detail following the description of the 1- and 2-zone partial equilibrium model.

1-Zone Partial Equilibrium Model

Model Assumptions - Figure III.B-2b shows the control volume used for the 1-zone partial equilibrium model. The primary difference between the total equilibrium model and the 1-zone partial equilibrium model is the addition of heterogeneous kinetics for devolatilization. Devolatilization is assumed to take place instantaneously with the yield and composition equal to the ultimate volatile yield and composition. The 2-step devolatilization model (2-S model, Kobayashi, 1976) or the functional group model (FG model, Solomon and Hamblen, 1985) are used to predict the ultimate volatile yield which is defined as the total volatile weight loss as time becomes large. Solid residence times on the order of one hour would justify this assumption. The FG model is used to predict devolatilization compositions including tar.

The devolatilization submodel also predicts the amount and composition of the ultimate char fraction. Dulong's formula is used to calculate the heating value of the char and Equations III.B-7 and 8 are used to calculate the heat of formation and sensible enthalpy of the char, respectively. As shown in Figure III.B-2b, tar is allowed to be recirculated into the reactor. The recirculated tar fraction is assumed to react with the other equilibrium gases. The tar recirculation fraction is specified by the user.

Devolatilization Submodels - The ultimate volatiles yield determined from the 2-S model as t becomes large (as $t \rightarrow \infty$) is:

$$Y^{\infty} = \frac{(Y_1 k_1 + Y_2 k_2)}{(k_1 + k_2)} \qquad \text{(III.B-11)}$$

where Y and k refer to the instantaneous yield of volatiles and Arrhenius rate constants, respectively. The subscripts refer to the low- and high-temperature reactions which describe the 2-S model. The predicted ultimate volatiles yield is a function of temperature.

The ultimate volatiles yield and composition for the FG model can be determined to be:

$$\omega_{i,c}^{\infty} = \begin{cases} 0. & \text{for all i except } CH_3OH,\ nvC, \text{ and } S_{org} \\ (1 - x^{\circ}) y_i^{\circ} & \text{for } CH_3OH,\ nvC, \text{ and } S_{org} \end{cases} \qquad \text{(III.B-12)}$$

$$\omega_{i,t}^{\infty} = \frac{x^{o} y_i^{o} k_t}{k_t + k_x} \qquad \text{(III.B-13)}$$

$$\omega_{i,g}^{\infty} = \left(1 - x^{o}\right) y_i^{o} + \frac{x^{o} y_i^{o} k_t}{k_t + k_x} \qquad \text{(III.B-14)}$$

where $\omega_{i,c}$, $\omega_{i,t}$, and $\omega_{i,g}$ are the ultimate weight fractions of char, tar and light gases that compose the i^{th} functional group, respectively. Other quantities in Equations III.B-12 through 14 are x^{o}, y_i^{o}, k_i, and k_x which represent the ultimate tar forming fraction, the initial fraction of the i^{th} functional group, distributed Arrhenius rate constant for the i^{th} functional group, and distributed Arrhenius rate constant for the tar, respectively. The subscripts CH_3OH, nvC, and S_{org} refer to the methanol, nonvolatile carbon, and organic sulfur functional groups, respectively. The ultimate volatiles composition predicted by the FG model is a function of temperature history.

The distributed rate constants were determined by a seven-point Gaussian-Legendre quadrature (Abramowitz and Stegun, 1972). Frequency factors, mean activation energies, and standard deviations of activation energies were obtained from Seric et al. (1987).

The 2-S model can be combined with the FG model to predict volatiles composition by the following equation:

$$x^{o} = 1 + \frac{\left[1 - \frac{(Y_1 k_1 - Y_2 k_2)}{(k_1 - k_2)}\right]}{\left(y_{MeOH}^{o} + y_{nvC}^{o} + y_{Sorg}^{o}\right)} \qquad \text{(III.B-15)}$$

The 1-zone partial equilibrium model has been programmed to use the 2-S model or FG model for yield. The FG model is used to predict volatiles composition for both the 2-S model and the FG model.

Solution Technique - Figure III.B-2b shows the control volume used for the 1-zone partial-equilibrium model. The ash temperature, well-mixed reactor temperature (or zero-dimensional temperature), and exit raw gas temperatures are assumed to be the same. Similar to the total equilibrium model, the daf coal is also assumed to completely react. Complete reaction of the daf coal is equivalent to assuming that the daf coal reacts completely either by devolatilization, gasification or oxidation. The total equilibrium model does

not differentiate between the mechanism for these chemical processes. However, the 1-zone, partial-equilibrium model allows devolatilization and drying to take place separately from gasification and oxidation reactions. Devolatilization and drying are assumed to occur at the same temperature as oxidation and gasification (this assumption is relaxed in the 2-zone, partial-equilibrium model). Furthermore, the mass evolved during drying and devolatilization is assumed to mix ideally with the equilibrium gases. Thus the model is designated a 1-zone, partial-equilibrium model as discussed previously.

Mathematically, the primary differences between the total-equilibrium model and the 1-zone, partial-equilibrium model are the energy and material balances around the gasification zone. The heat of devolatilization is assumed to be negligible. The sensible energy lost in the ash and energy lost through the wall are calculated similarly as in the total-equilibrium model discussed previously. The energy balance is identical to Equation III.B-1 except for the inclusion of tar recycle. The FG model predicts the total amount of tar produced by devolatilization. A fraction of the tar is allowed to be recirculated. The fraction of recirculated tar is specified by the user.

The solution technique for the 1-zone, partial-equilibrium model is as follows:

1. Guess the exit temperature, T_e.
2. Calculate quantities that depend on T_e (e.g. V^{∞}, ω_i, h_e, h_i, h_i°, Q, and h_g).
3. Calculate T_e, by material balance and equilibrium assumption.
4. Repeat 1-3 until guessed T_e equals calculated T_e.

1-Zone, Partial Equilibrium Model Results - Predictions of CO and H_2 in the gasifier effluent were slightly improved over the total equilibrium model. Exit temperature predictions were also improved. After comparing results from the two 1-zone models, it was decided to divide the gasifier into two temperature zones--a drying/devolatilization zone and an oxidation/gasification zone. Temperature resolution such as 2-zone or 1-D models should permit lower devolatilization temperatures and higher gasification/oxidation temperatures. Consequently, volatiles yield and composition will be different than 1-zone predictions. Also, the equilibrium

CO/CO_2 ratio increases with increasing temperature, leading to better agreement with measured effluent concentrations.

2-Zone Partial Equilibrium Model

Equations and Solution Technique - Figure III.B-2c shows the control volume used for the 2-zone partial equilibrium model. The primary difference between the 1-zone partial equilibrium model and the 2-zone partial equilibrium model is that devolatilization and drying are assumed to take place at the exit temperature, T_e, which is different than the equilibrium zone temperature, T_{eq}. Gasification and combustion are assumed to take place at the equilibrium temperature. The energy balances around the two zones are similar to previously discussed energy balances.

The solution technique for the 2-zone, partial-equilibrium model is as follows:

1. Guess the exit temperature, T_e.
2. Calculate quantities that depend on T_e (e.g. volatile yield and composition, enthalpy of char, and enthalpy of the tar).
3. Guess the equilibrium zone temperature, T_{eq}.
4. Calculate quantities that depend on T_{eq} (e.g. h_a^s, Q, and h_g).
5. Calculate T_{eq}, by material balance and equilibrium assumption.
6. Repeat 3-5 until guessed T_{eq} equals calculated T_{eq}.
7. Calculate T_e with energy balance around drying/devolatilization zone by using the secant method.
8. Repeat 1-7 until guessed T_e equals calculated T_e.

energy required for drying and sensible enthalpy of the feed coal are supplied to the drying/devolatilization zone. The wall heat loss as well as the sensible enthalpy loss in the ash is attributed to the equilibrium zone. In reality, these quantities should be partitioned between the two zones. The solution technique described above requires two iteration loops. Convergence for the 2-zone partial equilibrium model is on the order of seconds on a Sun-386i workstation computer.

Total Equilibrium and Partial Equilibrium Modeling Results

Westfield Predictions - Input parameters for the Westfield predictions were obtained from Elgin and Parks (1974). The predicted exit temperatures and compositions for the total-equilibrium, 1-zone partial-equilibrium, and 2-zone partial-equilibrium models are shown in Figure III.B-3. The Illinois No. 6 case also shows predictions from Yoon et al. (1978). Predictions from all equilibrium models are comparable to the predictions from the literature. The CO predictions for both 1-zone models are low, although the partial-equilibrium model is closer to measured values. CO predictions from the 2-zone model are even closer to measured values.

The most surprising results are the Rosebud predictions. The 1-zone models failed to give reasonable exit temperature or composition predictions. The exit temperatures were as much as 230 K higher than measured values. The 2-zone, partial-equilibrium model predicted the exit temperature for the Rosebud case to within 5 degrees Kelvin. The energy required to dry the coal and heat up the feed coal causes the temperature in the drying/devolatilization zone to be lower. The predicted compositions for the Rosebud case with the 2-zone, partial-equilibrium model were in close agreement with measured compositions.

Temperature Sensitivity to Steam/Oxygen Ratio - Figure III.B-4a show the effect of steam/oxygen on exit temperature for the equilibrium models. As expected, the exit temperature decreases with increasing steam. Figure III.B-4a also shows the temperature of the equilibrium zone predicted by the 2-zone model. The 1-zone exit temperature is bounded by the 2-zone exit and equilibrium temperatures. As the steam flow rate is increased, the difference between the exit temperature and equilibrium decreases. This effect may be due to less reactions taking place at the lower temperatures.

H_2/CO Sensitivity to Steam/Oxygen Ratio - Figure III.B-4b shows the effect of steam/oxygen on the exit molar ratio of H_2/CO. The total-equilibrium model predicts a monotonic increase in the H_2/CO ratio with increasing steam/oxygen. The partial-equilibrium model gives an S-shaped curve with the H_2/CO ratio approaching a limit of approximately 10. Figure III.B-4c shows data from various coals from Rudolph (1978). All of the equilibrium models seem to predict the correct trend. The 2-zone model seems

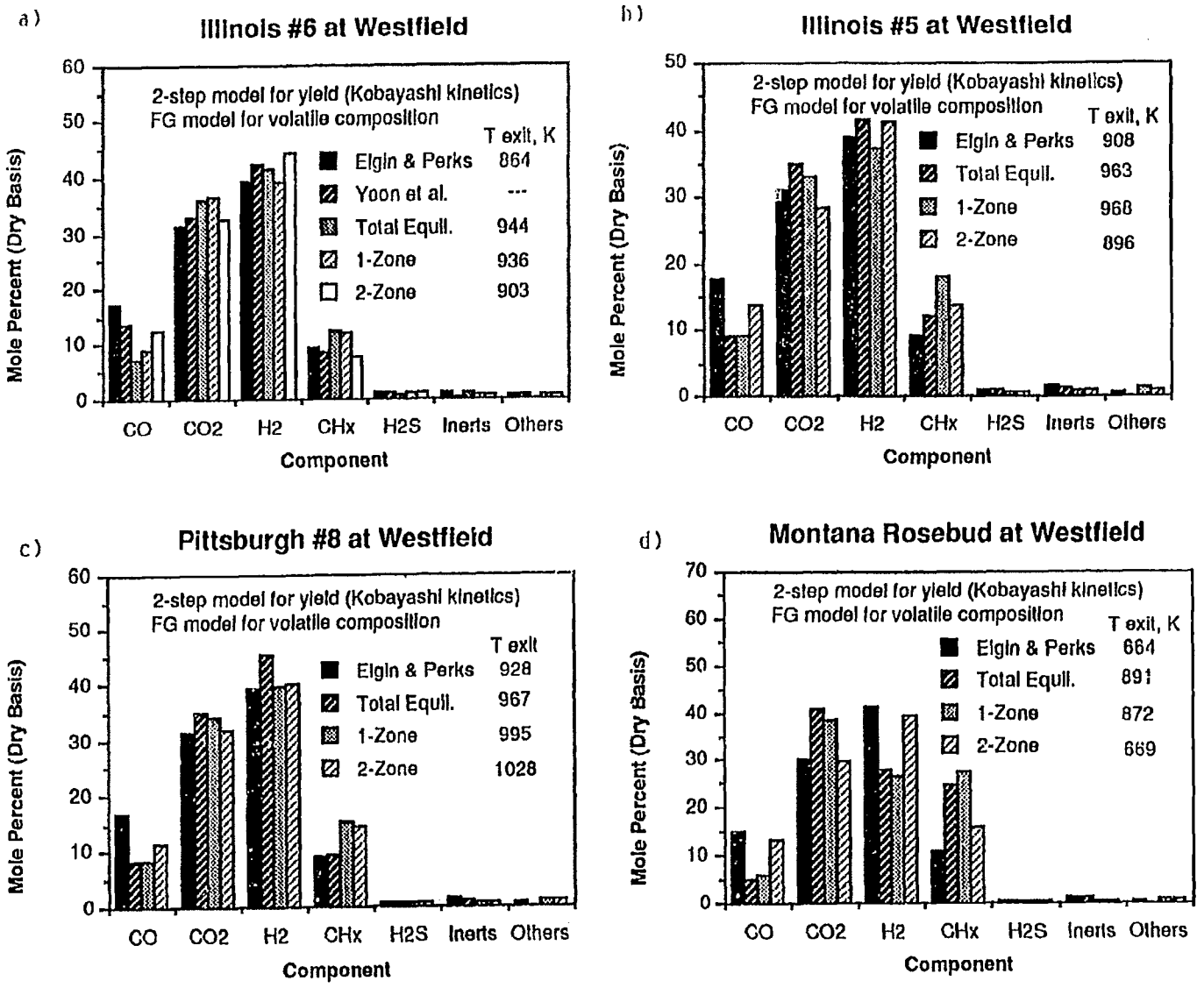

Figure III.B-3. Westfield American Coal test predictions a) Illinois No. 6, b) Illinois No. 5, CO Pittsburg #8, and d) Montana Rosebud.

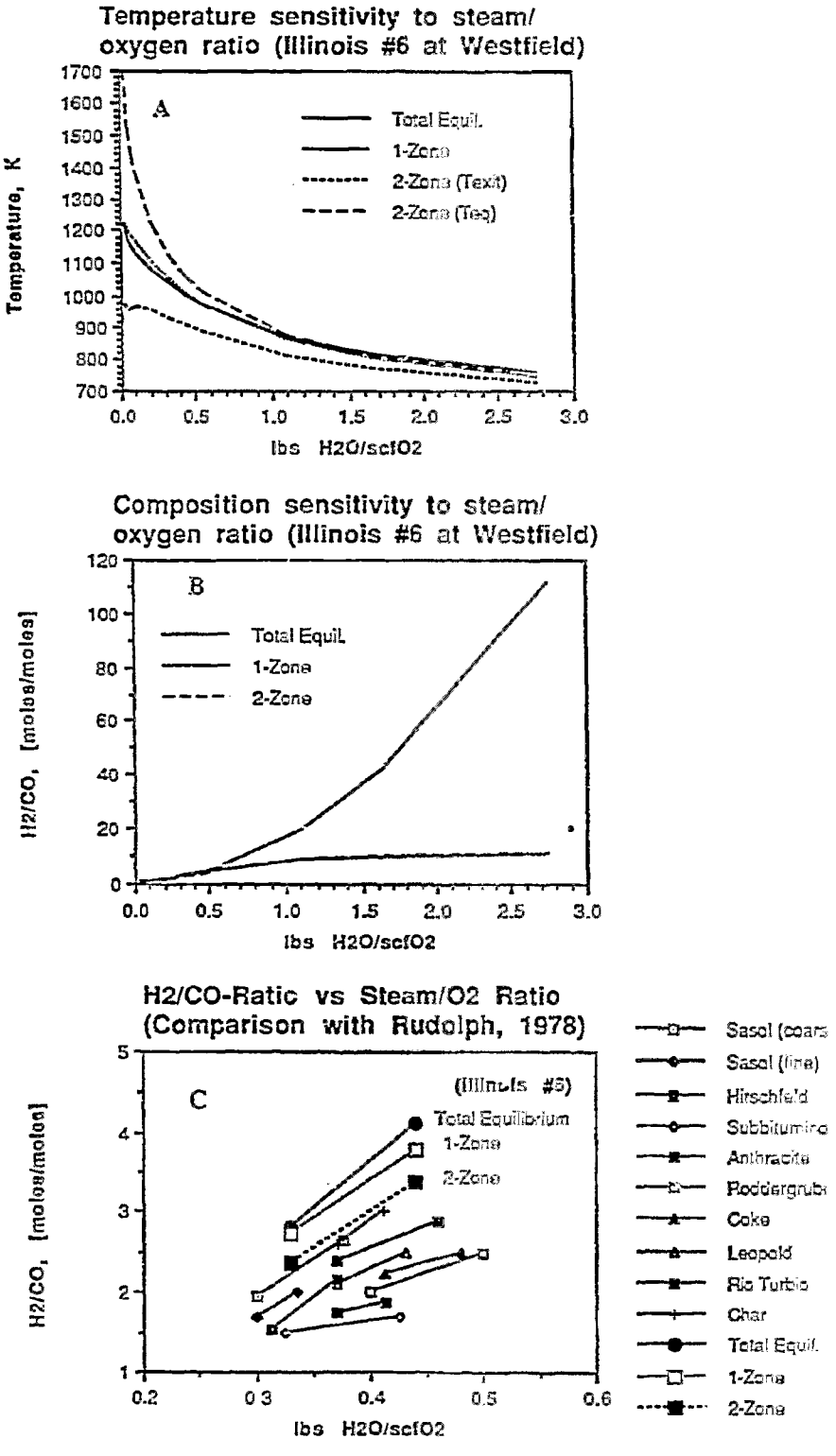

Figure III.B-4. Temperature and composition sensitivity to steam/oxygen ratio.

equilibrium models seem to predict the correct trend. The 2-zone model seems to give better absolute values for the H_2/CO ratio.

Effect of Pressure on Raw Gas Composition - Figure III.B-5 shows the effect of gasification pressure on the composition of the raw exit gas. The influence of pressure is most noticeable for the total equilibrium model. The addition of devolatilization tends to dampen out the influence of pressure. This can be explained by the fact that the FG model was developed primarily for small particles. There are no particle size or pressure effects in the model. Large-particle submodels being developed under Subtask 2.e should provide particle size and pressure effects for the equilibrium codes.

Significance of Equilibrium Submodels

The equilibrium chemical submodel options have provided additional insight into the moving-bed process. Justification for development of accurate large-particle submodels that predict the effects of pressure and particle size has been demonstrated. Accurate effluent predictions can be made by providing additional spatial resolution. All equilibrium models predict adequate raw gas compositions with best results from the 2-zone, partial-equilibrium model The 2-zone model will be used to provide an accurate exit temperature and concentration guess for the 1-D model.

Plans

Heterogeneous gasification and oxidation kinetics will be coded into the 2-zone, partial-equilibrium model. The interface between kinetics and equilibrium will be investigated further. Differences between global equilibrium and local equilibrium will be explored. A simplified version of the FG-DVC model for large particles provided by AFR will be coded into the 2-zone, partial-equilibrium model. After obtaining sufficient experience with the chemical submodels to be used in the moving-bed code, development of the 1-D, moving-bed code will be initiated. The 1-D code will include the FG model, 2-S model and simplified version of the large-particle, FG-DVC model, a simplified char oxidation/gasification submodel based on the shell-progressive or ash-segregation submodels, and a gas-phase chemistry submodel based on partial equilibrium.

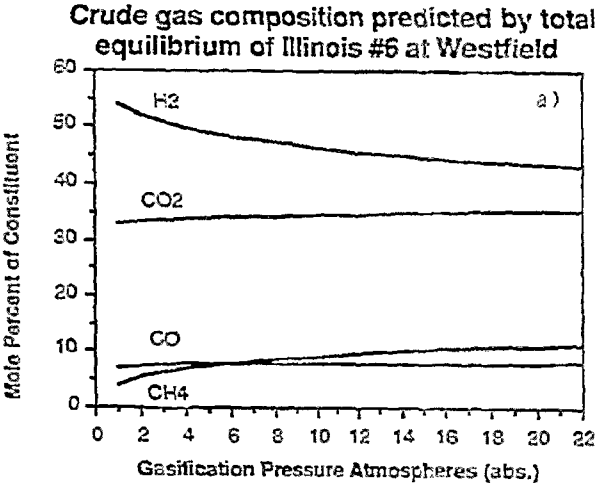

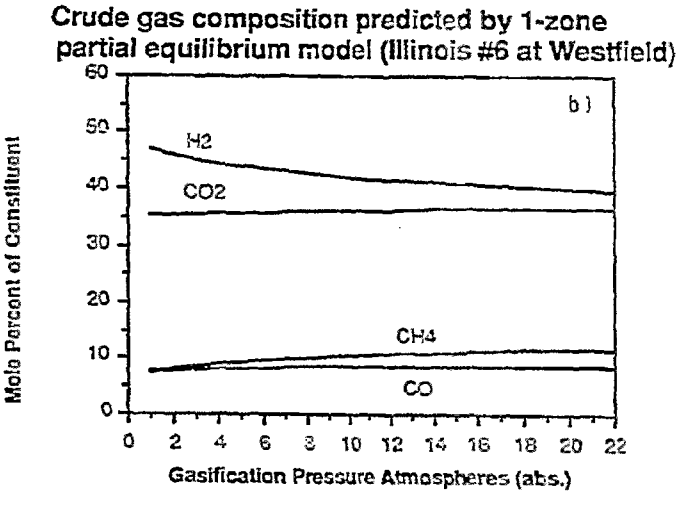

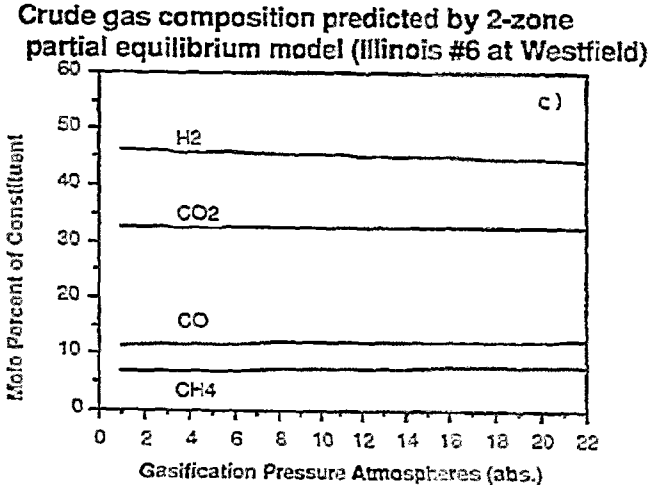

Figure III.B-5 Effect of pressure on raw gas composition with a) 1-zone total equilibrium model b) 1-zone partial equilibrium model and c) 2-zone partial equilibrium model.